A Statistical Analysis of the Relationships among Rainfall, Outgoing Longwave Radiation and the Moisture Budget during January–March 1979*

MARK L. MORRISSEY

Department of Meteorology, University of Hawaii, Honolulu, HI 96822

(Manuscript received 27 July 1985, in final form 5 November 1985)

ABSTRACT

An analysis of the statistical relationships among observed daily rainfall, outgoing longwave radiation (OLR) and the moisture budget (precipitation minus evaporation or $P - E$), obtained from three independent data sources during January through March, 1979, indicates that on a daily basis $P - E$ and OLR correlate significantly better with each other than they do with observed rainfall over open-ocean regions where the spatial density of rainfall observing stations is low. A spatial correlation over the Pacific Ocean indicates that $P - E$ and OLR correlate well in most—but not all—highly convective regions where both variables have moderate to high variances, and are uncorrelated in dry regions. Low correlations are obtained in regions of shallow convection and in areas of weak moisture convergence with cirrus at upper levels.

It is demonstrated that OLR, $P - E$, or observed rainfall alone cannot properly define the areal extent of large scale convective activity. A technique is developed in which $P - E$ is used in conjunction with OLR to better establish the intensity and spatial bounds of large-scale convective activity.

1. Introduction

Researchers often use rainfall, outgoing longwave radiation (OLR) and the moisture budget (calculated precipitation minus evaporation or $P - E$) as indicators of convection, particularly for the investigation of temporal and spatial characteristics of large-scale (>500 km) deep convective activity (hereafter referred to as LSCA) (Murakami, 1980; Yanai et al., 1973; Zangvil, 1975). In order to properly define the time and space scales of LSCA using observed rainfall, OLR, or $P - E$, it is necessary to understand the physical relationships among these variables and to identify their associations with LSCA.

Recently, several researchers compared data obtained from satellite observations to observed open-ocean rainfall. Meisner and Arkin (1984) constructed a precipitation index which uses satellite infrared imagery to obtain rainfall estimates which are then correlated with observed station rainfall. Kilonsky and Ramage (1976) developed a technique which relates visual satellite imagery to observed rainfall. Studies such as these use observed station rainfall as an accurate measure of convection, to which other convective variables are compared. This study will show, however, that open ocean observed rainfall, although a good indicator of localized convection, is not an accurate measure of LSCA, especially when considering synoptic time and space scales. This question is discussed further in section 5.

The main objective of the present paper is to examine the physical relationships among rainfall, OLR, and $P - E$ using a detailed statistical analysis of daily data obtained from three independent data sources over an extensive region of the central Pacific (37.5°N to 37.5°S, and 120°E to 120°W).

In section 3 a spatial comparison of three-month time-mean OLR and $P - E$ is made and in section 4 a time-space variance comparison of OLR and $P - E$ is performed. Due to the sporadic locations of rainfall observation stations over the Pacific Ocean a spatial comparison with rainfall was precluded. However, a temporal comparison of all three variables is done in section 5.

2. Data and computational procedures

This study utilizes daily (0000 GMT) values of u, v, ϕ, r, T at seven pressure levels (1000, 850, 700, 500, 300, 200, 100 mb) for the period 1 January to 31 March 1979. These data were extracted from the objectively analyzed FGGE (First GARP Global Experiment) level IIIb data set prepared by the European Centre for Medium Range Weather Forecasts (ECMWF) at a reduced resolution of 3.75° longitude-latitude intervals over a region extending from 120°E to 120°W and 37.5°N to 37.5°S.

Twice daily OLR obtained from NOAA polar orbiting satellites are digitized on a 2.5° × 2.5° grid and resolution is reduced to 3.75° × 3.75° longitude-latitude intervals. Daily OLR was obtained by averaging the twice daily values (0330 LST, 1530 LST).

Daily rainfall data are extracted from FGGE IIc surface-based precipitation data sets for various Pacific area rainfall stations and are time smoothed using a

* Contribution Number 85-02 of the Dept. of Meteorology, University of Hawaii.

three-point weighted moving average in an effort to reduce small deviations in data recording times at each station.

The horizontal u and v wind components and the geopotential height (ϕ) in the FGGE data set were the basic objectively-analyzed fields. Temperature T was determined from the initialization procedure; the initialized temperature is very sensitive to the numerical model used at ECMWF (Lubis and Murakami, 1984). A study by Murakami et al. (1984) showed that the numerical model used to determine the temperature has questionable accuracy in certain regions and during certain periods and therefore affects the quality of the mixing ratio estimates; this is also shown below.

FGGE level IIb station moisture data provide the basis of level IIIb moisture analyses. A simple successive approximation scheme (not an optimum interpolation scheme) was used at ECMWF for the analyses of layer mean moisture. Since the moisture data in FGGE level IIb observations are not significantly better than those available for the FGGE IIa data set, the resulting moisture analysis is biased towards the forecast model used to provide the first guess. This is especially true for the period from December 1978 to April 1979. (A better description of the problems associated with FGGE moisture analyses is given in FGGE Newsletter No. 1, 1983). Therefore the FGGE level IIIb moisture analyses were not well-handled and are of questionable accuracy, especially over data-void regions. The data-sparse areas of concern include the east-central and southeast Pacific regions which are almost devoid of stations (FGGE Operations Report, 1980). A rather complete investigation of the accuracy of statistics calculated from FGGE data is given by Lorenc and Swinbank (1984).

It has also been noted in the literature that the ECMWF FGGE moisture computations for the tropics for low levels are too dry by about 1–2 gm kg^{-1} (Lambert, 1983). However, as will be shown in sections 3 and 4, FGGE level IIIb moisture data appear to be adequate for describing the relative temporal and spatial fluctuations (i.e., comparing positive vs negative regions and relative strengths of different spatial patterns) of the large scale (>500 km) moisture fields over most of the tropical Pacific. Therefore the reader should keep in mind the inaccuracies in the moisture data and should concentrate on the qualitative rather than quantitative results of this study.

In the FGGE level IIIb data set, relative humidity is determined from the mean-layer water content and the initialized temperature. The mixing ratio q is calculated from the temperature T and relative humidity r. The mixing ratio at a given pressure level used in the $P - E$ calculations given here is given by

$$q = 0.622r(e_s/p), \tag{1}$$

$$\ln e_s = 21.6 - (5410/T), \tag{2}$$

where e_s and p represent the saturation vapor pressure and the pressure, respectively, at a given pressure level. Equation (2) is derived from the Clausius-Clapeyron equation with the latent heat of vaporization equal to 2.500×10^6 J kg^{-1}, the specific gas constant for water vapor of 461.7 J kg^{-1} and a saturation vapor pressure of 6.11 mb at 273.155 K.

$P - E$ is calculated here by the following:

$$P - E = -1/g\left(\int_{P_{tp}}^{P_s} \partial q/\partial t dP\right) - 1/g\left(\int_{P_{tp}}^{P_s} \nabla \cdot q\mathbf{V} dP\right) - 1/g\left(\int_{P_{tp}}^{P_s} \partial q\omega/\partial P dP\right),$$

(A) (B) (C)

where P_s = surface pressure, P_{tp} = 300 mb, $\mathbf{V}$ is the horizontal velocity, ω the vertical velocity in pressure coordinates, g the gravitational acceleration (9.8 m s^{-2}) and t time. Surface pressure is calculated from the geopotential height (ϕ) of 1000 mb using the hydrostatic equation. Due to the availability of q and $\mathbf{V}$ only at discrete pressure levels, values of these variables at these standard levels (1000, 850, 700, 500 and 300 mb) represented layer-mean estimates (i.e., q at 850 mb represents the layer mean q from 925 to 775 mb). The integrals were evaluated using a trapezoidal rule from P_s to P_{tp}. Term A represents the rate of change in the storage of moisture and is important when considering daily time scales. Term B denotes the net horizontal moisture convergence into a column of air, while term C is the net vertical convergence of moisture flux. Term C, which is neglected in the $P - E$ calculation, integrates to zero over open-ocean regions (assuming vertical velocity is zero at the surface level), but could be significant when considering mountainous terrain.

Divergent wind fields for the tropics calculated from ECMWF IIIb u and v data have been reported to be suspect, especially on horizontal scales less than 1500 km (Julian, 1984). Lubis and Murakami (1984), however, showed good agreement between the spatial patterns of integrated moisture divergence (using ECMWF IIIb data) and a convective index developed by Murakami (1983) over the Pacific Ocean from 1 December 1978 to 3 February 1979. (The convective index incorporates, primarily, infrared (IR) imagery from satellites for its construction, and will be further discussed in section 8.) Julian (1984) compared spatial patterns of the divergent wind (calculated from the velocity potential) to OLR while considering OLR to be an absolute measure of the strength of convection. This study will show that OLR is not necessarily an absolute measure of convection and its use must be carefully considered. Due to the difficulty of testing the accuracy of the divergent wind, the quality of the final $P - E$ estimate, (a function of wind divergence) will be critically examined in sections 3 and 4.

To help compmensate for small inaccuracies in the FGGE wind data a divergence correction term, based on the conservation of mass, is applied to the $P - E$ calculations and is given by

$$\nabla \cdot \mathbf{V}_{\text{corrected}} = \nabla \cdot \mathbf{V}_{\text{calculated}} + \left(\int \nabla \cdot \mathbf{V} dP \right) \Big/ (P_s - P_1),$$

where $P_1 = 100$ mb.

In addition, $P - E$ is time and space smoothed (see the Appendix for an explanation of the spatial smoothing function) over all grid points to eliminate unwanted small-scale fluctuations (noise) in the FGGE data.

To help verify the reliability of the $P - E$ estimates, four-times daily surface observations (0000, 0600, 1200 and 1800 GMT, including plotted ship and land station models) are utilized for the January to March, 1979 period (hereafter referred to as the study period). The surface observations were plotted by National Weather Service personnel based in Honolulu, Hawaii. Surface observations are used in this study to qualitatively evaluate convective situations over selected areas of the Pacific by identifying cloud and precipitation type. Assessments of the convective situation for various regions are compared to those inferred from $P - E$ and OLR values. (Refer to section 3.)

Because of the qualitative nature of data extracted from the surface observations, the area represented by each ship or island observing station varied with visibility. For instance, on a clear day a ship weather observer might report trade-wind cumulus with precipitation within sight and thus could be reporting for an area of approximately 2000 km^2 (assuming the observer can see 25 km in all directions). Since we were primarily interested in large-scale (>500 km) convective situations, all regions selected for investigation using the surface observations were required to have, per day, at least one observation for every 250 000 km^2 of the region and the observations within the region have to be somewhat uniformly spatially distributed. (In this paper, exceptions were occasionally made to this criterion, based upon a subjective assessment of the synoptic situation.) This station density is the minimum necessary for the surface observations to adequately represent the large-scale convective situation within the selected region.

3. Outgoing longwave radiation vs $P - E$: Time-mean relationship

Time-mean charts of OLR and $P - E$ for 1 January to 31 March 1979 are presented in Figs. 1 and 2, respectively. (Note: all figures are for the time period 1 January to 31 March 1979, except where indicated.) The following features are noted:

1) A large area of positive $P - E$ and low OLR (<240 W m^{-2}) values (which is the approximate radiation emitted by cold, high-level clouds) extend poleward from the equator to roughly 20°S and from 120°E eastward to approximately 150°W. This area corresponds to a highly convective region associated with the Southern Hemisphere summer monsoon and the southern Pacific Convergence Zone (SPCZ), which extends east and southeast from 170°E to 150°W (Vincent, 1982; Ramage, 1975; Davidson et al., 1984).

A survey of the January to March surface observations was conducted for two subset areas of this region: Area A, encompassing an area of suspected strong convection within the monsoon region, extends from the equator to 15°S and from 150° to 170°E. Area B, encompassing another area of suspected strong convection, this time in the SPCZ region, extends from 155° to 135°W and from 15°S to 30°S. Areas A and B were selected because of the numerous ship and station observations in each area (>20 observations per day for each region) and their proximity to actively convective regions [positive $P - E$ and low OLR (<240 W m^{-2})].

During the study period, an average of 47 and 32% of the total observations per day included precipitation in areas A and B, respectively. Greater than half of the observations reporting precipitation in both areas A and B indicated heavy showers or thunderstorms.

2) Relatively poor association between OLR and $P - E$ is observed over a region north of 25°N and extending eastward from 120°E to 120°W. Isolated moisture convergence and high level cirrus associated with midlatitude frontal systems, which travel eastward through this area during January to March, are primarily responsible for this lack of agreement.

3) Low OLR (<240 W m^{-2}) and negative $P - E$ values over an area east of Hawaii extending from 140° to 120°W and from 30° to 15°N are the result of frequent large-scale cirrus surges accompanied by relatively dry lower levels associated with large-scale cloud intrusions from the tropics (Anderson and Oliver, 1970). For this region (area C), an average of 12% of the surface observations per day reported precipitation during the study period (from an average of 17 total observations per day). The precipitation reported was primarily light rain and drizzle. The most often reported cloud types were fair weather cumulus with scattered or dense cirrus, occasionally accompanied by middle cloud.

Thus, the surface observations are in agreement with the assessment from the three-month $P - E$ estimate that this region was dry and not highly convective during the study period.

The lack of association of $P - E$ with OLR in this region illustrates the major difficulty with OLR when used as an indicator of the intensity and spatial extent of LSCA. Outgoing longwave radiation cannot accurately distinguish cirrus directly overlying (and produced by) active, deep convection from large areas of cirrus directly overlying nonconvective conditions.

The averaged OLR values (see Fig. 1) in area C and in area B (mentioned in subsection 3a) are similar (be-

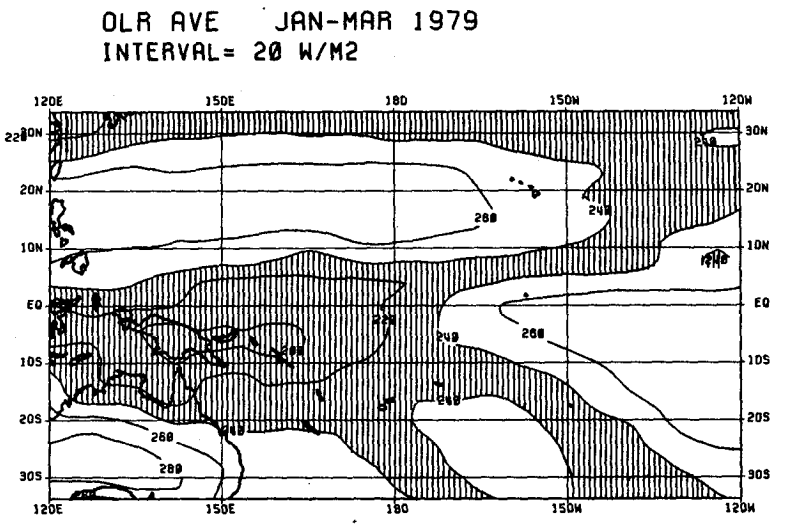

FIG. 1. Time-mean chart of OLR from 1 January to 31 March, 1979. Shading indicates regions where OLR is less than 240 W m^{-2}.

tween 240 and 230 W m^{-2}), but the convective situation is very different. The obtained values of 12 and 32% of surface observations reporting precipitation per day for the present region and area B, respectively are significantly different at the 99% confidence limit, suggesting very different mean convective conditions in both regions.

This weakness in OLR for accurate evaluation of convective activity due to cirrus overlying nonconvective conditions will be referred to in this paper as "cirrus contamination" of OLR.

4) Near 10°N, 125°E, weak low-level moisture convergence and wide spread shallow convection, associated with the low-level northeast monsoon flow through this region, are responsible for the positive $P - E$ and high OLR values (>240 W m^{-2}) (Flores and Balagot, 1969).

The surface observations indicate primarily continuous light rain and drizzle for this region.

5) A large area of positive $P - E$ values and high OLR (>240 W m^{-2}) extends from 140° to 120°W and from 10°N south to 5°S. This region corresponds to the climatological position of the Central Pacific Near-Equatorial Convergence Zone (Ramage et al., 1981).

Unfortunately, the convective situation during the study period (and thus the $P - E$ values for the region)

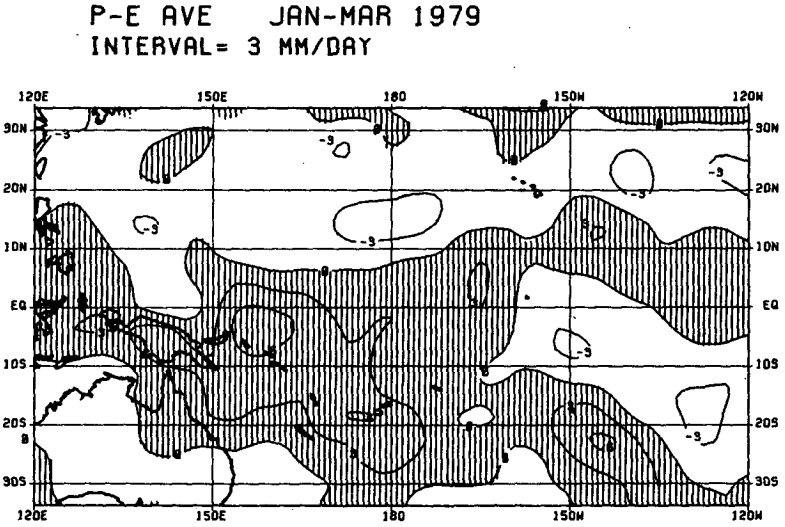

FIG. 2. Time-mean chart of $P - E$ from 1 January to 31 March, 1979. Shading indicates regions where $P - E$ is greater than 0 mm d^{-1}.

cannot be verified due to the scarcity of ship observations in this area; therefore, nothing more will be said about this region.

Thus, it is apparent from Figs. 1 and 2 that over many regions OLR and $P - E$ alone cannot satisfactorily define the nature and spatial extent of LSCA, and more importantly, it should not be assumed that OLR is always inversely proportional to LSCA.

4. $P - E$ vs OLR: Time-space variance relationships

It may have been assumed that an estimate of the quality of $P - E$ could be obtained from the strength of its correlation with OLR. On the other hand, low correlation values do not necessarily indicate the low quality of the $P - E$ estimate due to various physical relationships between clouds and convection. This was discussed previously and is amplified further as follows.

Figure 3 shows daily $P - E$ correlated with daily OLR at each grid point for January through March. Shaded areas indicate regions where the correlation coefficient is less than -0.3. (A correlation coefficient of -0.3 is significantly different from a coefficient of 0.0 at the 99% confidence limit.) A close examination of this chart indicates that $P - E$ correlates reasonably well (< -0.3—that is, a linear relationship is established with OLR) within the Southern Hemisphere summer monsoon region (10°–20°S from 135° to 170°E) and the SPCZ (roughly 25°S from 170°E to 135°W). The correlation is also fairly strong southwest of Hawaii where upper-level troughs occasionally induce low-level convergence-generating strong convection (Atkinson, 1971). Thus the $P - E$ estimate is apparently sufficient to describe the daily fluctuations in large-scale moisture convergence at least over actively convective regions where the correlation coefficient is less than -0.3.

Small positive correlation coefficients centered near 25°N, 140°W again correspond to the region of large-scale cirrus contamination as described in section 3.

In dry, cloudless regions, where there is little precipitation, evaporation is not thought to correlate well with large values of OLR. (Outgoing longwave radiation is basically a measure of sea surface temperature in cloudless oceanic regions.) This is because evaporation at the sea surface is a function of many daily varying factors other than sea surface temperature, such as surface wind speed, moisture and air temperature (Gill, 1982). Thus $P - E$ is not correlated well with OLR in areas such as 150°E, 20°N and 20°N, 170°E which are regions of general subsidence and moisture divergence (Atkinson, 1971) (hence $P - E < 0$ mm day^{-1} and OLR > 240 W m^{-2}) where evaporation accounts for most of the variance in $P - E$.

The spatial distribution of the standard deviation values for both OLR and $P - E$, calculated at each grid point for the study period, are shown in Figs. 4 and 5, respectively. Comparing these figures with Fig. 3, one can observe that in highly convective regions both OLR and $P - E$ have large standard deviations and correlate significantly well. This is illustrated by the significant correlation (< -0.3) and large standard deviation values (>32 W m^{-2} for OLR and >6 mm day^{-1} for $P - E$) of both variables along the monsoon region (the upper-level trough region near Hawaii and the SPCZ). An exception to this relationship between standard deviation and correlation is discussed as follows.

A curious area of low correlation values exist over New Guinea which is a region that surface observations

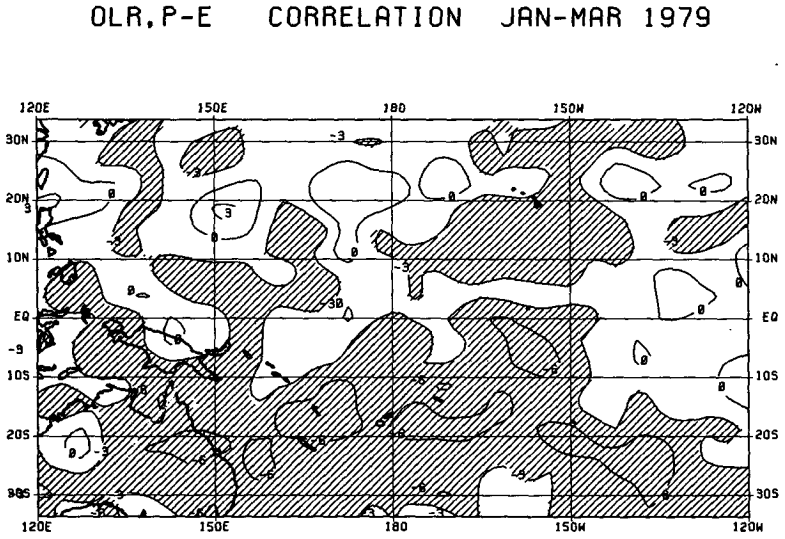

FIG. 3. Spatial distribution of the correlation r of $P - E$ vs OLR calculated at every grid point. Units are $r \times 10$. Shading indicates regions where the correlation is less than -0.3.

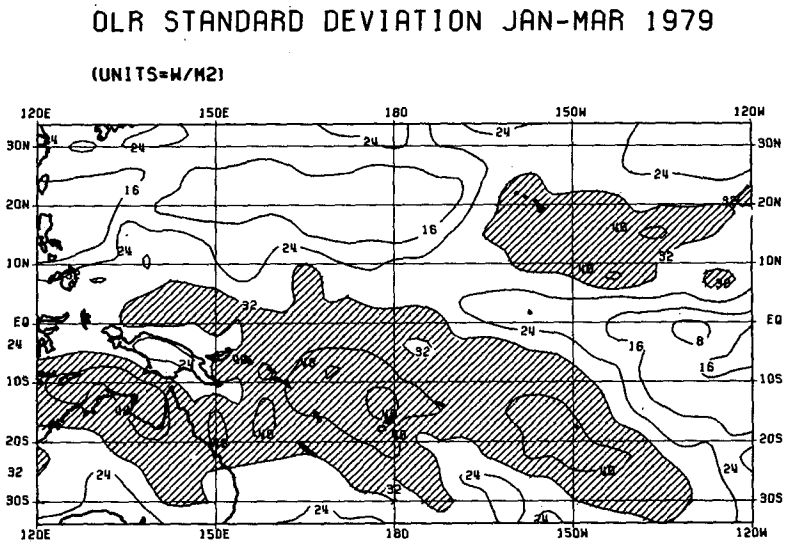

FIG. 4. Spatial distribution of the standard deviations of OLR calculated at every grid point.

suggest is strongly convective (not shown). An examination of the spatial distribution of standard deviations for both variables (see Figs. 4 and 5) show relatively low OLR standard deviation values (<32 W m^{-2}) and moderate $P - E$ standard deviation values (>4 mm day^{-1}) over this region. I suspect that the low correlation values over this region could be due to many orographically induced short-lived convective cells embedded in a persistent cirrus deck (thus the low OLR and moderate $P - E$ variances in this region). This cirrus deck is most likely created from the almost continuous vertical moisture transport from the numerous cumulonimbus clouds associated with the summer monsoon. Thus cirrus contamination of OLR can be a problem even in moist regions.

Some error might be introduced here by the neglect of term C in the $P - E$ calculation (refer to section 2) which could become important when considering mountainous terrain. Also, the moisture convergence due to these short-lived convective cells must occur around 0000 GMT to be measured by the once-daily FGGE measurements used in the $P - E$ calculations. Therefore, due to diurnal biases and questionable data quality, care must be taken in assuming confidence in these low correlation values. However, the physical reasons suggested for these correlations are certainly

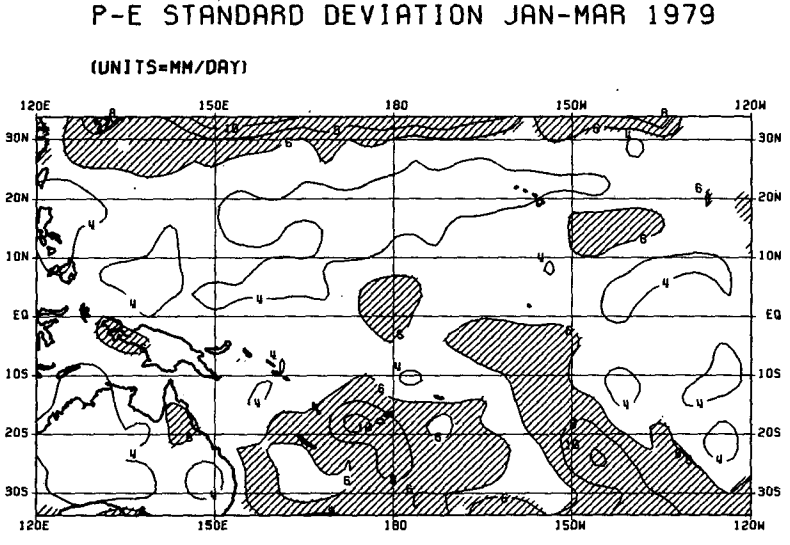

FIG. 5. As in Fig. 4 but for $P - E$.

possible and should be considered when utilizing short-term convective variables in the study of large scale convection.

5. Time-variance comparison of open-ocean rainfall, $P - E$ and OLR

As was mentioned in the Introduction, due to the sporadic locations of rainfall stations in the central Pacific a general spatial comparison of observed rainfall with $P - E$ and OLR is precluded. However, a temporal comparison of the three variables can be made over some selected regions.

A representative open-ocean area was chosen in which the enclosed daily observed rainfall, $P - E$, and OLR values were areally averaged and compared statistically for the period January through March, 1979. A correlation coefficient was calculated for each pair of variables. Each coefficient turned out to be statistically significant at the 99% level and, therefore, linear relationships were established for each case.

In conducting such a comparison a geographical area encompassing a number of rainfall stations was selected so that the station density was comparable to the $P - E$, OLR grid point density in that area. Only atoll rainfall stations were chosen in order to minimize the orographic effect. Also, rainfall stations with missing data during the study period were avoided and, to be meaningful, the selected area was situated in an actively convective region.

The region selected (hereafter referred to as study region I) contains the atoll rainfall stations Beru (1°S, 175°E), Funafuti (8°S, 179°E), and Nanumea (5°S, 176°E). This represents an area of 4.92×10^5 km^2 (see Fig. 6) and is a region where OLR and $P - E$ are well correlated (Fig. 3).

a. *Rainfall vs $P - E$*

The rainfall vs $P - E$ correlation coefficient obtained for study region I was 0.36. The variable-time plot of the observed rainfall vs $P - E$ relationship is shown in Fig. 7. Despite the statistically significant correlation coefficient, poor agreement is often observed during the period, especially from days 45 to 80 when the areally averaged daily rainfall and $P - E$ estimates are low.

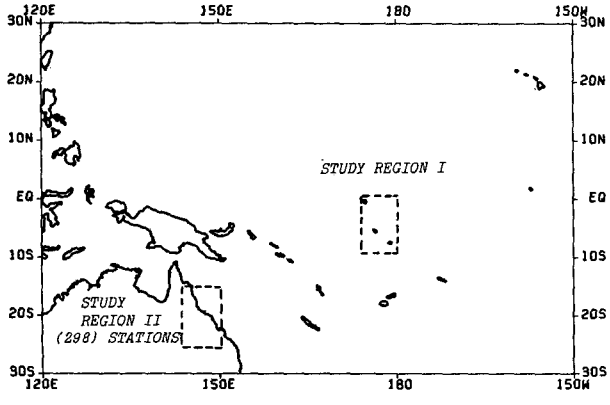

FIG. 6. Geographical location of the study regions I & II of island rainfall stations. The regions are indicated by dashed lines. Station locations in study region I are indicated by heavy dots.

Several factors which might influence the $P - E$ vs observed rainfall daily relationship are suggested:

1) Inaccuracies in daily rainfall values are certainly possible, although this is extremely difficult to ascertain.

As mentioned in section 2, the moisture and divergent wind analyses for the FGGE IIIb data set is of questionable accuracy over data void regions. However, as mentioned above, $P - E$ does correlate significantly well (< -0.3) with OLR in this region (Fig. 3). This indicates that $P - E$ does, in fact, respond to changes in convective activity in this region and suggests that qualitative assessments of the $P - E$ vs OLR rainfall relationships are of some value.

2) The spatial distribution of rainfall stations in the study area is quite uniform (see Fig. 6) and the station density (number of stations per area) is equal to that of the $P - E$ grid point density (three-grid points in the study area). Examination of daily rainfall values (not shown) shows large variations among stations. Due to the nature of tropical LSCA, which consists of many individual convective cells with space and time scales on the order of 10 km and a few hours respectively, observed rainfall at a given station is a measure of localized convection rather than a measure of large-scale convection. In order for observed rainfall to accurately represent LSCA, station density would have to be quite large. Thus, the validity of observed rainfall as a measure of LSCA is extremely sensitive to station density.

$P - E$ is derived from large-scale field variables (u, v, ϕ, T, r) and is therefore not as dependent on the number of observations per area.

3) In the tropics where the daily variances of humidity and, to a lesser degree, wind speed (Atkinson, 1971), are small, fluctuations in evaporation rates are also suspected to be fairly small. In highly convective areas, such as study region I, precipitation is believed to account for most of the variance in $P - E$, although this is difficult to verify. One estimation of the daily fluctuations in evaporation rates can be made by observing that the standard deviation values of $P - E$ (see Fig. 4) in dry regions (where $P - E < 0$ mm day^{-1} in Fig. 2; i.e., 180°E, 20°N) are generally less than 4 mm day^{-1}.

4) As mentioned in section 4, there may also be considerable diurnal biases in the $P - E$ estimates because the input parameters (u, v, T, ϕ, r) of $P - E$ are measured only once a day while rainfall measurements, on the other hand, are integrated daily values.

b. *$P - E$ vs OLR*

The correlation coefficient obtained in this case is -0.67. Note that the correlation coefficient here rep-

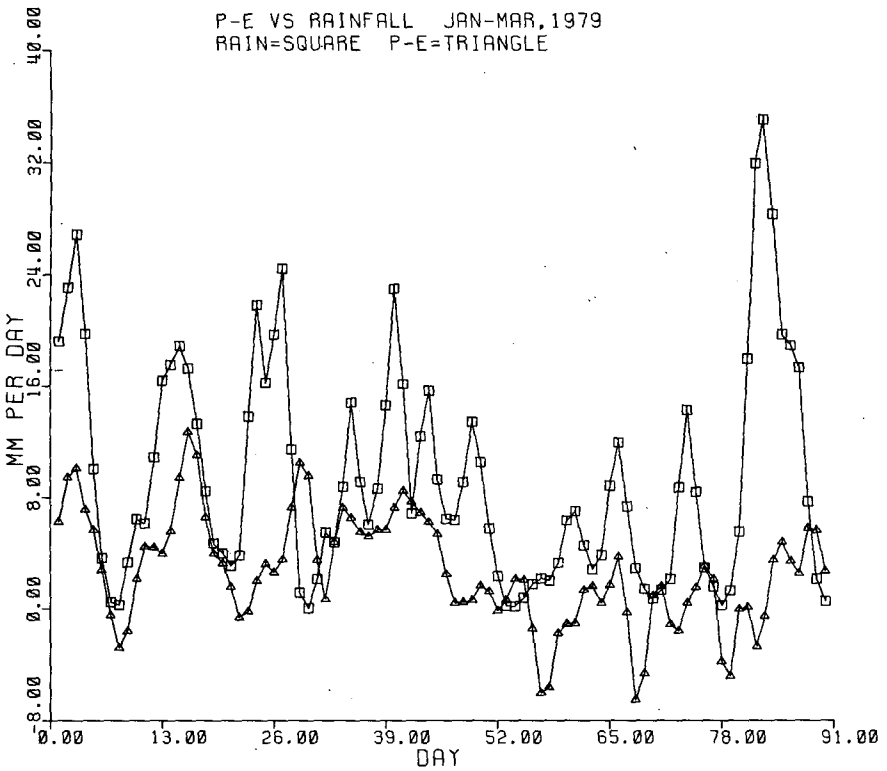

FIG. 7. 1 January to 31 March plot of $P - E$ vs observed rainfall for study region I.

resents the areal averaged OLR and $P - E$ estimates within study region I as opposed to the correlations at individual grid points as in Fig. 3. The variable-time plot is shown in Fig. 8. Factors which might influence the $P - E$ vs OLR relationship in the study area include

1) Moderately high variances of both $P - E$ and OLR exist in this region during the study period (see Figs. 4 and 5). As demonstrated earlier, $P - E$ usually correlates well with OLR in areas where there are large variations in strong convective activity.

2) Both OLR and $P - E$ are averaged over the same grid points. This is probably of minor importance due to the relatively low spatial variance of OLR and $P - E$ within this region.

c. Rainfall vs OLR

The correlation coefficient obtained is −0.52. The variable-time plot is shown in Fig. 9. Suggested factors which could influence this relationship are as follows:

1) The undetermined accuracy of the observed station rainfall estimates and low rainfall station density within the study region (as discussed in subsection 5a) appear to severely limit the observed rainfall's measurability of large-scale deep convection.

2) A scatter plot of OLR vs observed rainfall (not shown), shows a large amount of scatter throughout the range of both variables. This could reflect the effects of cirrus contamination of OLR and the large amount of spatial variability in the observed rainfall data due to local effects. Diurnal biases in the twice per day OLR measurements also contribute to this scatter.

6. Testing the relationships

The correlations between the variables were tested for statistical significance using the standard normal test of the null hypotheses H_0: $r_1 = r_2$, H_0: $r_2 = r_3$ and H_0: $r_3 = r_1$ at the 95% confidence level where

1) $r_1 = 0.36$; the $P - E$ vs observed rainfall correlation coefficient.

2) $r_2 = 0.52$; the absolute value of the observed rainfall vs OLR correlation coefficient.

3) $r_3 = 0.67$; the absolute value of the $P - E$ vs OLR correlation coefficient.

The results of the test indicate that

1) H_0: $r_1 = r_2$ cannot be rejected. (Therefore r_1 is not significantly different than r_2.)

2) H_0: $r_2 = r_3$ is rejected.

3) H_0: $r_1 = r_3$ is rejected.

Therefore, $P - E$ and OLR correlate better with each other than they do with rainfall during the study period. The major factor which may be responsible for this is

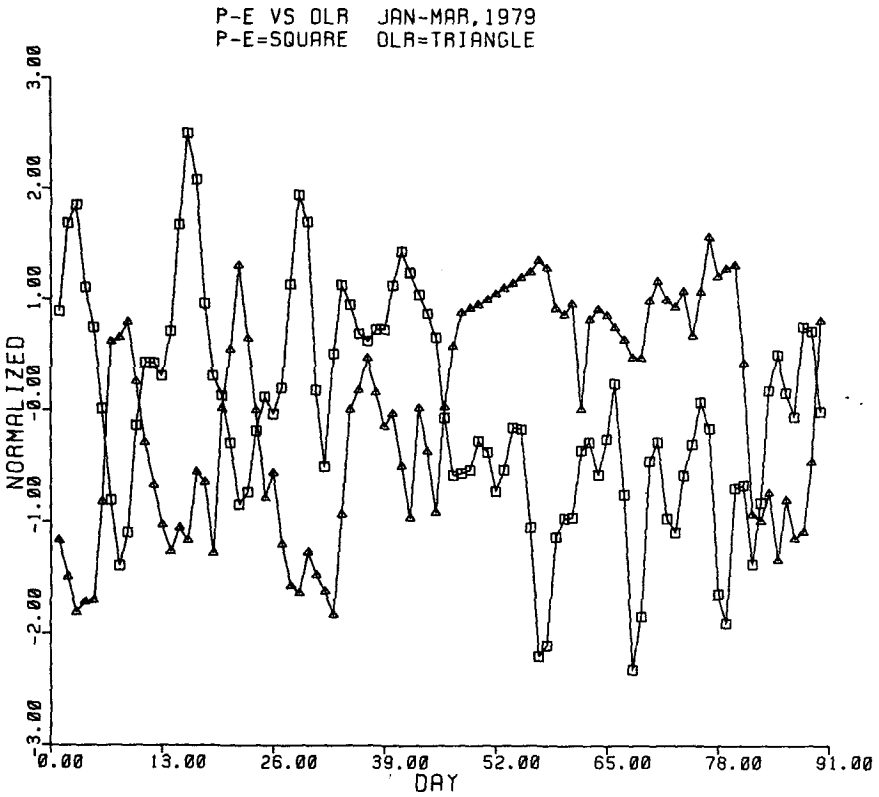

FIG. 8. 1 January to 31 March plot of $P - E$ vs OLR for study region I. Data are normalized by subtracting the mean and dividing by the standard deviation.

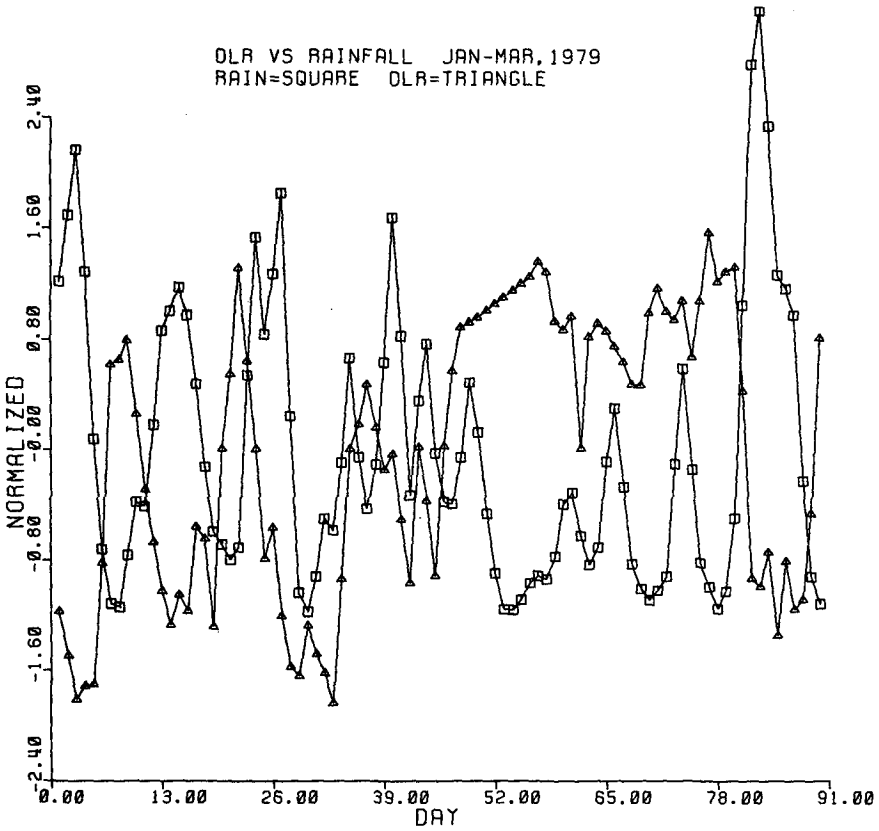

FIG. 9. As in Fig. 8 but for OLR vs observed rainfall.

the low station density of rainfall observing stations within the study region.

To investigate this further a second study region was selected having the same total area and OLR and $P - E$ grid point density as the original study region, but with a greatly increased number of rainfall observing stations. Study region II is located over the highly convective region of northern Australia (see Fig. 6) and encompasses 298 stations. The correlation coefficient for $P - E$ and observed rainfall for this study region for the January to March period is 0.85. This value is significantly greater than the $P - E$, observed rainfall correlation coefficient obtained for study region I (0.36). The $P - E$, OLR correlation is -0.65 and the OLR, observed rainfall correlation is -0.64, neither of which is significantly different than their respective correlations obtained for study region I. The $P - E$, observed rainfall correlation is significantly different than both the $P - E$, OLR and OLR, observed rainfall correlations. This indeed indicates that the low rainfall station densities over open ocean precludes the use of open-ocean rainfall as an accurate measure of LSCA and helps to support the validity of $P - E$ as a measurement of the large-scale fluctuations in precipitation (where data quality can be verified). Also, the strong correlation coefficient obtained for $P - E$, observed rainfall in study region II suggests that the error due to diurnal biases in the $P - E$ estimate becomes less when considering large-scale moisture convergence.

7. Spatial extent of cirrus contamination

As the results of this study indicate, cirrus contamination of OLR can seriously limit the usefulness of OLR as a measure of LSCA. Precipitation minus evaporation, although probably a better indicator of LSCA, cannot always accurately locate LSCA, as can seen from the time-mean chart of $P - E$ over the Philippine area (see Fig. 2), where there are high amounts of low-level moisture convergence and widespread shallow convection. The combination of daily OLR and $P - E$, however, helps to better define the intensity and spatial extent of LSCA, therefore isolating the spatial extent of cirrus contamination in OLR as well. The procedure is to identify moist ($P - E > 0$ mm day^{-1}) and dry ($P - E < 0$ mm day^{-1}) regions where OLR is less than 240 W m^{-2}. Either $P - E$ or OLR can be contoured. The choice depends on the accuracy of the $P - E$ estimate. As shown in sections 3 and 4, $P - E$ appears to be adequate for describing the relative temporal and spatial fluctuations of the large-scale moisture convergence fields. However, as mentioned in section 2, little confidence should be placed in the absolute accuracy of the $P - E$ estimate derived from the FGGE data set. Therefore, until better quality data can be utilized, OLR, not $P - E$, should be contoured, using OLR to estimate the intensity of convection. With OLR contoured, $P - E$ is used only to identify dry and moist regions of low OLR. The threshold value of OLR (240 W/m^2) is used by many authors to delineate convective regions from nonconvective regions (Murakami, 1980; Lau and Chan, 1983). Lau and Chan (1983) compared threshold OLR values with frequency distributions of highly convective clouds using a method developed by Kilonsky and Ramage (1976). They found that their results were not very sensitive to the exact value of the threshold used, provided it was in the 230–250 W m^{-2} range. A sample output for the $P - E$, OLR method with $P - E$ contoured is shown for 6 February 1979 in Fig. 10. In Fig. 11, the method is again shown for 6 February but with OLR contoured. Comparisons with visual satellite imagery and radiosonde and surface data for selected days and regions help validate this procedure for investigating convective vs nonconvective areas over the Pacific Ocean.

As illustrated in Fig. 10, large areas of cirrus contamination in tropical regions are evident. By identifying (per day) what percentage of the area enclosed by OLR less than 240 W m^{-2} is also associated with negative $P - E$ values, and then averaging these percentages for the study period, we find a daily average of approximately 34% of the area enclosed by OLR less than 240 W m^{-2} over the Pacific ocean is nonconvective. (Due to the uncertainty in the $P - E$ estimates and the diurnal biases in both OLR and $P - E$, this value should be used as a qualitative estimate only.) Thus, cirrus contamination in the tropics should not be ignored, especially on a daily basis.

8. Concluding remarks

Results of this study indicate that the tendency for observed rainfall to be a measure of localized convection makes its usefulness as an indicator of LSCA very dependent on station density. Therefore, the very low station density, together with the sporadic locations and varying data reporting times between rainfall stations over the central Pacific, suggest that observed rainfall may not be an accurate indicator of the time and space scales of open ocean LSCA. Thus, careful consideration is required when utilizing observed daily rainfall as a measure of LSCA.

Physical explanations for the statistical relationships obtained suggest that OLR alone does not always adequately describe convective conditions and that $P - E$ combined with OLR helps to minimize the inadequacies of both variables for the identification of LSCA.

The technique which combines $P - E$ with OLR provides us with a descriptive tool with which to study LSCA. When moisture flux data become more reliable they will provide a better measure of convective intensity. With the presently available FGGE data set, the technique can spatially isolate large-scale cirrus contamination which is the major complaint with OLR over open ocean areas, especially on daily time scales.

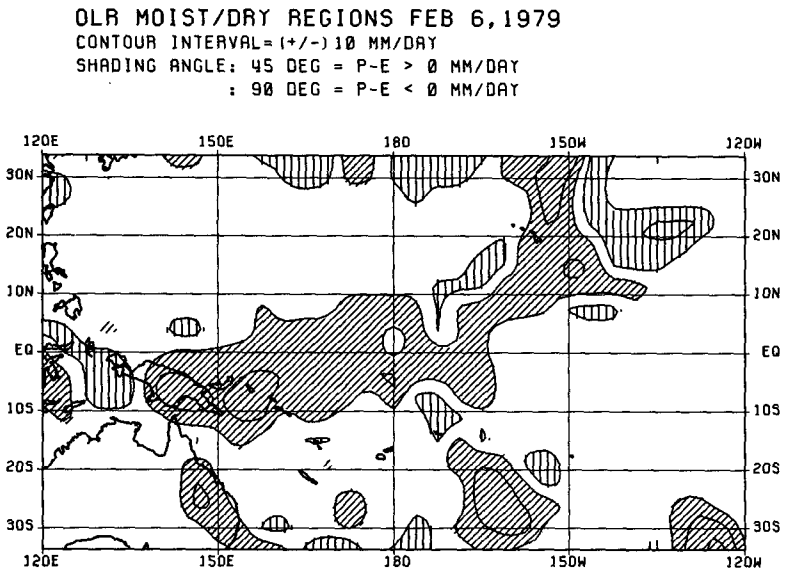

FIG. 10. Moist and dry regions of low OLR for 6 February 1979. Shading angled at 45° indicates regions where OLR is less than 240 W m^{-2} and $P - E$ is greater than 0 mm d^{-1}. Shading angled at 90° indicates regions where OLR is less than 240 W m^{-2} and $P - E$ is less than 0 mm d^{-1}. Data are contoured in units of $P - E$ (mm d^{-1}).

Other authors have attempted to deal with the problem of cirrus contamination of satellite obtained longwave radiation. Murakami (1983) using irradiance (IR) data observed by GMS–1 geostationary satellite indicated that strong convection could be isolated by assuming that regions with large temporal variances of IR correspond to regions of LSCA. As can be observed from Fig. 4, the standard deviation of OLR over the area surrounding New Guinea during the study period is rather low (<32 W m^{-2}) and would thereby indicate an absence of strong convection using Murakami's method. Averaged $P - E$ and OLR (see Figs. 1 and 2) together with the surface observations indicate strong convection for the region. This discrepancy can be explained by a large persistent cirrus canopy which possibly exists over this region (thus low IR standard deviation values) during the active phase of the Southern Hemisphere monsoon (January to March). As mentioned earlier, this cirrus canopy can be produced by continuous large-scale vertical moisture transport, which in turn is caused by the large number of convective "hot towers" inherent in the monsoon. It would, therefore, be very difficult to distinguish the areas of active convection in the high-level cirrus deck over this region using OLR exclusively. The $P - E$, OLR combination helps to overcome this difficulty by effectively looking "below" the high-level cirrus clouds and thus can better assess the convective situation.

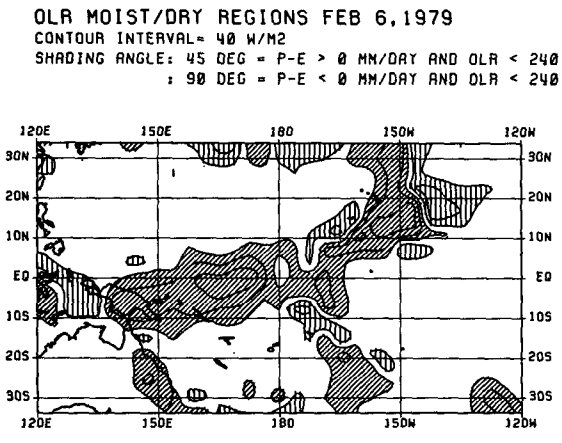

FIG. 11. As in Fig. 10 but data are contoured in units of OLR (W m^{-2}).

Acknowledgments. The author would like to thank Dr. Takio Murakami for his help and advice, to Mrs. Dixie Zee for lending her computer expertise and Mr. Kelcy Chang for his help with the surface observations. Discussions with Dr. Colin Ramage, Dr. Thomas Schroeder, Mr. Mark Lander, Mr. Jose Maliekal, Mr. W. L. Sumathipala and Dr. Susan Postawko are gratefully acknowledged. This research was completed as part of the author's dissertation. The author would like to thank NOAA for funding this research under Grant NA 80 RAH 00002.

APPENDIX

Spatial Smoothing Function

The spatial smoothing function for $P - E$ consists of a five-point weighted average and is given by

$$r(i, j) = [r(i + 1, j) + r(i - 1, j) + r(i, j + 1) + r(i, j - 1) + 4.0*r(i, j)]/8.0,$$

$r(i, j) = P - E$ estimate at grid point (i, j),

$$i = 1, 2, 3 \cdots 33, j = 1, 2, 3, \cdots 19.$$

Index values (i, j) represent grid points $3.75° \times 3.75°$ apart in the zonal and meridional directions, respectively.

REFERENCES

Anderson, R. K., and V. J. Oliver, 1970: Some examples of the use of synchronous satellite pictures for studying changes in tropical cloudiness. *Ext. Abstracts: Symp. Tropical Meteorology,* Honolulu, Amer. Meteor. Soc., EXII1–EXII6.

Atkinson, G. D., 1971: *Forecasters' Guide to Tropical Meteorology.* Tech. Rep. 240, Air Weather Service, USAF, 240 pp.

Davidson, N. E., J. L. McBride and B. J. McAvaney, 1984: Divergent circulations during the onset of the 1978–1979 Australian monsoon. *Mon. Wea. Rev.,* **112,** 1684–1696.

Flores, J. F., and V. F. Balagot, 1969: Climate of the Philippines. *World Climate Survey,* **8,** Elsevier, 159–213.

FGGE Newsletter, 1983: No. 1, May, USC–GARP, JH 810, [Nat. Acad. Sci., 2101 Constitution Ave., Washington, DC., 20418,] 33 pp.

FGGE Operations Report, 1980: Observing System Operations, 1 December 1978–30 June 1979. *The Global Weather Experiment, Vol. I.* GARP Rep., ICSU and MO, [Nat. Acad. Sci., 2101 Constitution Ave.,, Washington, DC., 20418,] 78 pp.

Gill, A. E., 1982: *Atmosphere–Ocean Dynamics.* Academic Press, 661 19–38.

Julian, P. R., 1984: Objective analysis in the tropics: A proposed scheme. *Mon. Wea. Rev.,* **112,** 1752–1767.

Kilonsky, B. J., and C. S. Ramage, 1976: A technique for estimating tropical open-ocean rainfall from satellite observations. *J. Appl. Meteor.,* **15,** 972–975.

Lambert, S. J., 1983: List of known or suspected problems with the ECMWF analyses of FGGE data. FGGE Newsletter No. 1, May 1983, USC–GARP, JH 810, Nat. Acad. Sci., 2101 Constitution Ave., Washington, DC., 20418.

Lau, K., and P. H. Chan, 1983: Short-term variability and atmospheric teleconnections from satellite-observed outgoing longwave radiation. Part I: Simultaneous relationships. *Mon. Wea. Rev.,* **40,** 2735–2750.

Lorenc, A. C., and R. Swinbank, 1984: On the accuracy of general circulation statistics calculated from FGGE data—a comparison of results from two sets of analyses. *Quart. J. Roy. Meteor. Soc.,* **110,** 915–942.

Lubis, S. M., and T. Murakami, 1984: Moisture budget during the 1978–79 Southern Hemisphere monsoon. *J. Meteor. Japan,* **62,** 748–760.

Meisner, B. N., and P. A. Arkin, 1984: The GOES precipitation index: Large scale tropical rainfall estimates using infrared data. *Proc. 15th AMS Tech. Conf. Hurricanes and Tropical Meteorology,* Miami, Amer. Meteor. Soc., 203–206.

Murakami, T., 1980: Empirical orthogonal function analysis of satellite observed outgoing long-wave radiation during summer. *Mon. Wea. Rev.,* **108,** 205–222.

——, 1983: Analysis of the deep convective activity over the western Pacific and Southeast Asia, Part I: Diurnal variation. *J. Meteor. Japan,* **61,** 60–75.

——, T. Iwashima and T. Nakazawa, 1984: Heat, moisture, and vorticity budget before and after the onset of the 1978–79 Southern Hemisphere Summer Monsoon. *J. Meteor. Japan,* **62,** 69–87.

Ramage, C. S., 1975: *Monsoon Meteorology.* Academic Press, 296 pp.

——, S. J. S. Khalsa and B. N. Meisner, 1981: The Central Pacific Near-Equatorial Convergence Zone. *J. Geophys. Res.,* **86,** 6580–6598.

Vincent, D. G., 1982: Circulation features over the South Pacific during 10–18 January 1979. *Mon. Wea. Rev.,* **110,** 981–993.

Yanai, M., S. Esbensen and J. Chu, 1973: Determination of bulk properties of tropical cloud clusters from large-scale heat and moisture budgets. *J. Atmos. Sci.,* **30,** 611–627.

Zangvil, A., 1975: Temporal and spatial behavior of large-scale disturbances in tropical cloudiness deduced from satellite brightness data. *Mon. Wea. Rev.,* **103,** 904–920.